Journal of Clinical Pharmacology and Therapeutics

ISSN: 2766-8347

Research Article

Inhibition of Pkcβ II Alleviates Renal Ischemia-Reperfusion Injury by Suppressing Ferroptosis in Mice

Maodi Gong[1], Hua Shi[1], Yikun Wu[2], Yuangao Xu[1], Guangyi Hong[2], Wei Chen[1] and Shuxiong Xu[1]*

[1]*Department of Urology, Guizhou Provincial People's Hospital, China*

[2]*School of Medicine, Guizhou University, China*

Abstract

Renal Ischemia-Reperfusion (I/R) injury can cause renal insufficiency, leading to the need for renal replacement therapy in severe cases, placing a substantial burden on patient recovery and life. Mitigating renal I/R injury is a current research focus. Protein kinase C (PKC) isozymes, with PKCβII as the primary isoform in the kidney, are crucial protein kinases. Ferroptosis plays a vital role in acute kidney injury resulting from renal I/R. This study aimed to explore the involvement of PKCβII in renal I/R and its potential association with iron-induced cell death. Using a mouse renal I/R model, the study examined the impact of various pretreatment approaches, including Ruboxistaurin (a PKCβII inhibitor) and Erastin (an ferroptosis agonist), on renal injury. The study also delved into the role of PKCβII in iron-induced cell death and its potential mechanisms. The findings indicate that PKCβII is activated during renal I/R, and inhibiting PKCβII activation improves renal dysfunction and tissue damage. Furthermore, iron-induced cell death is markedly increased in renal I/R injury, and PKCβII inhibition can mitigate ferroptosis by suppressing the PKCβII/ACSL4 pathway. In summary, the results propose that PKCβII may contribute to mediating renal I/R injury, and targeted inhibition of PKCβII activation could emerge as a novel therapy for improving renal I/R injury.

Keywords: Renal ischemia-reperfusion injury; Ferroptosis; PKCβ II; Lipid peroxidation

Introduction

When the kidney surpasses its tolerance for ischemia, reperfusion can result in damage, causing renal Ischemia-Reperfusion (I/R) injury. In clinical practice, the prevalence of renal I/R injury is high and can ultimately lead to chronic kidney disease or end-stage renal disease, imposing a substantial impact on healthcare and the economy [1,2]. Consequently, preventing and treating renal I/R injury remains a crucial focus in medical research.

Protein Kinase C (PKC) is a phospholipid- and Ca^{2+}-dependent serine/threonine protein kinase involved in vital cellular signal transduction [3,4]. During I/R injury, the release of endogenous catecholamines increases, activating α1-adrenergic receptors and the G protein-phospholipase C-mediated signal transduction pathway. This pathway promotes phosphatidylinositol catabolism, yielding inositol triphosphate (IP3) and Diacylglycerol (DG). IP3 induces intracellular Ca^{2+} release, while DG activates Na^+/H^+ exchange *via* PKC activation. This process elevates Na^+/Ca^{2+} exchange proteins, leading to heightened cytosolic and mitochondrial Ca^{2+} concentrations. Excessive mitochondrial Ca^{2+} uptake serves as the physiological basis for ferroptosis in renal cells during I/R [5]. PPKC isozymes, widely distributed in various tissues and organs, include PKCβII as the major isoform in the kidney [6]. Hence, we hypothesize that PKCβII may play a crucial role in renal I/R injury. Ferroptosis, a form of iron-dependent cell death, is initiated by the excessive accumulation of iron ions and lipid peroxidation [7]. Studies suggest that ferroptosis plays a pivotal role in acute kidney injury resulting from renal I/R [8]. Consequently, inhibiting ferroptosis is considered a significant strategy for preventing and treating renal I/R injury. Notably, the literature lacks reports on the role of PKCβII-mediated ferroptosis in renal I/R injury.

Therefore, this study established a mouse model of renal I/R injury to observe changes in renal PKCβII post-I/R. Subsequently, the PKCβII inhibitor Ruboxistaurin and the ferroptosis agonist Erastin were employed for intervention, allowing observation of changes in renal injury and ferroptosis. The study further explored the involvement of PKCβII-regulated ferroptosis in renal I/R injury. The anticipated results of this study aim to offer novel insights for preventing and treating renal I/R injury.

Materials and Methods

Animal model of renal I/R injury

Adult male C57BL/6 mice (20-21g), sourced from Chongqing Tengxin Laboratory Animal Co., Ltd., and housed in a specific pathogen-free facility at Guizhou Medical University (Guiyang, China), were employed. Mice were randomly divided into five groups based on distinct pretreatment methods: sham-operated treatment group (S), I/R treatment group (I/R), PKCβII inhibitor administration group (R+I/R), ferroptosis agonist administration group (E+I/R), and PKCβII inhibitor combined with ferroptosis agonist Erastin administration group (R+E+I/R). The R+I/R and R+E+I/R

Citation: Gong M, Shi H, Wu Y, Xu Y, Hong G, Chen W, et al. Inhibition of Pkcβ II Alleviates Renal Ischemia-Reperfusion Injury by Suppressing Ferroptosis in Mice. J Clin Pharmacol Ther. 2024;5(3):1063.

Publisher Name: Medtext Publications LLC

Manuscript compiled: Dec 02nd, 2024

***Corresponding author:** Shuxiong Xu, Professor of medicine, Department of Urology, Guizhou Provincial People's Hospital, No.83, East Zhongshan Road, Guiyang, Guizhou, China, Tel: 86-17785816723; Fax: 86-0851-85273772*

groups received 10 mg/kg of the PKCβII inhibitor Ruboxistaurin (MedChemExpress, NJ, USA) through preoperative gavage once daily for three days. The E+I/R and R+E+I/R groups were administered 30 mg/kg of the ferroptosis agonist Erastin (MedChemExpress, NJ, USA) through intraperitoneal injection. The remaining groups were treated with an equivalent volume of saline using the same methods (Figure 1). The Ruboxistaurin dosage was adjusted as previously described [9,10], and Erastin dosing followed earlier studies [11,12]. Subsequently, all mice were anesthetized, and a midline abdominal incision was made to carefully separate bilateral renal clips [13]. Twenty-four hours after reperfusion, mice were euthanized, and blood samples were collected for subsequent renal function testing. Kidneys were obtained, with a portion fixed in 4% paraformaldehyde and paraffin-embedded. Another portion was rapidly stored at -80°C for RNA extraction and protein analysis. A 1mm³ tissue block was also fixed in 1% glutaraldehyde and prepared for electron microscopy.

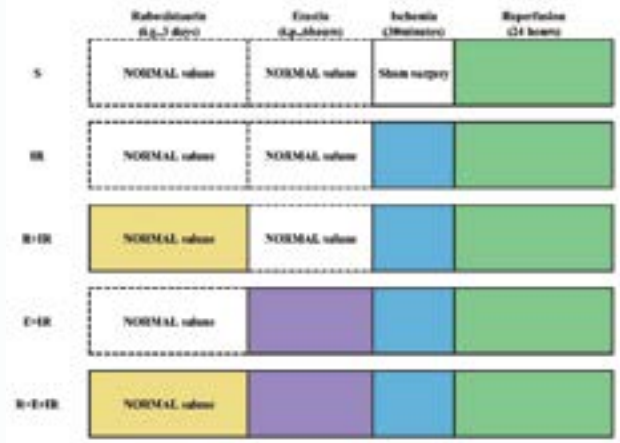

Figure 1: Handling measures for renal I/R mice. (S, IR, E+IR, W+IR, E+W+IR represent the surgery group, the I/R group, the Ruboxistaurin-treated I/R group, the Erastin-treated I/R group, and the Ruboxistaurin and Erastin combined treatment I/R group, respectively).

Renal function measurement

Creatinine assay kit (BioAssay Systems, NC, USA) and urea assay kit (Nanjing Jiancheng Co., Ltd., China) were utilized to determine Serum Creatinine (Scr) and Blood Urea Nitrogen (BUN), respectively, following the manufacturer's instructions.

Histopathological evaluation of the kidney

Paraffin sections of 2-μm kidney tissue were subjected to hematoxylin-eosin (H&E) staining, and the histomorphology was examined under a light microscope (BX53, Olympus, Tokyo, Japan). Renal pathological damage was assessed following the criteria outlined by Paller, et al. [11,14]. Briefly, 10 randomly selected views of each specimen (totaling 100 tubules) were scored based on the following criteria: 1 point for dilated tubules with flattened epithelial cells, 2 points for the presence of tubular patterns in the tubular lumen, 1 point for the presence of exfoliated necrotic cells without tubular patterns or cellular debris, 1 point for vacuolation of tubular epithelial cells, 1 point for nuclear consolidation of epithelial cells, and 0 points for normal tubules. If two or more of these pathological changes coexisted in the same tubule, the highest damage score was assigned. The final score for each specimen was based on the scoring of 100 tubules.

Detection of mitochondrial morphology in renal tissue

Blocks measuring 1 mm × 1 mm × 1 mm were obtained from mouse kidney tissue, pre-fixed with 3% glutaraldehyde, refixed with 1% osmium tetroxide, dehydrated stepwise in acetone, embedded in Epon 812, and semi-thin sections were stained with toluidine blue for optical positioning. Ultra-thin sections were prepared using a diamond knife, stained with uranyl acetate and lead citrate, and mitochondrial morphology was examined using transmission electron microscopy. Images were captured and recorded.

Immunohistochemistry

Sections of renal cortical tissue, measuring 4 μm in thickness, were treated with 3% hydrogen peroxide for 10 minutes to deactivate endogenous enzymes. Subsequently, the sections were incubated overnight at 4°C with appropriate primary antibodies, namely anti-Kim-1 (1:100, Abcam, MA, USA) and NGAL (1:50, Santa Cruz Biotechnology, TX, USA). Afterward, the sections were incubated with horseradish anti-rabbit or goat anti-mouse polyclonal antibodies (1:200, Abcam) for 30 minutes at room temperature. Positive expression of the aforementioned proteins in renal tubular epithelial cells was observed in ten fields of view under a light microscope at ×400 magnification. Optical density values were analyzed using Image-ProPlus 6.0 (Media Cybernetics Inc., MD, USA) software.

Western blot analysis

Total kidney protein was extracted, separated by sodium dodecyl sulfate-polyacrylamide gel electrophoresis (SDS-PAGE), and then transferred to Polyvinylidene Difluoride (PVDF) membranes (Millipore, MA, USA). Following closure with 5% milk powder for 2 hours at room temperature, the PVDF membranes were incubated overnight at 4°C with anti-PKCBII (1:2000, ABclonal), anti-ACSL4 (1:1000, ABclonal), anti-GPX4 (1:1000, ABclonal), anti-SLC7A11 (1:2000, ABclonal), and anti-TFRC (1.1000, Abcam) antibodies. Subsequently, the membranes were incubated with horseradish peroxidase-conjugated goat anti-rabbit IgG (1:600, Beyotime) or anti-mouse IgG (1:600, Proteintech Group, Inc.) for 2 hours at room temperature. Finally, the PVDF membranes were treated with enhanced chemiluminescence reagent (ECLPlus, Thermo Fisher Scientific) for 5 minutes. Protein bands were visualized using a chemiluminescence imaging system (Gene GnomeXRQ, Syngene, Cambridge, UK) and quantified using ImageJ software (Rawak Software Inc., Stuttgart, Germany).

Measurement of the levels of GSH、MDA、SOD and Fe^{2+}

Kidney tissues from each sample were homogenized in pre-cooled saline, and the levels of GSH, MDA, SOD, and Fe^{2+} were determined in the kidney tissue homogenates using specific assay kits obtained from Elabscience (Wuhan, China). The GSH assay kit (E-BC-K030-M), the MDA assay kit (E-BC-K025-M), the SOD assay kit (E-BC-K020-M), and the Fe^{2+} assay kit (E-BC-K773-M) were utilized for the accurate quantification of GSH, MDA, SOD, and Fe2+ levels in renal tissue homogenates.

Statistical analyses

GraphPad Prism 8.0.2 (GraphPad Software, CA, USA) was employed for statistical analysis, and the results were presented as mean ± Standard Deviation (SD). One-way Analysis of Variance (ANOVA) was utilized for group comparisons. A significance level of *P<0.05 was considered statistically significant.

Results

PKCβII mediates renal dysfunction and tissue damage due to renal I/R

In exploring the association between PKCβII and renal I/R injury, we initially assessed renal injury by examining Scr and BUN levels, the expression of renal injury markers (Kim1 and NGAL), and the renal pathology score. Scr and BUN levels, Kim-1 and NGAL expression, and tubular injury scores were elevated in the I/R group compared to the S group (Figure 2a-e). Additionally, PKCβII protein expression increased in the I/R group compared to the S group (Figure 3a and b). Following intervention with the PKCβII inhibitor Ruboxistaurin, the I/R+R group exhibited reduced Scr and BUN levels, Kim-1 and NGAL expression, and tubular injury scores compared to the I/R group. Moreover, PKCβII protein expression was also diminished in the R+I/R group. These findings suggest that PKCβII plays a role in mediating I/R-induced renal dysfunction and tissue damage.

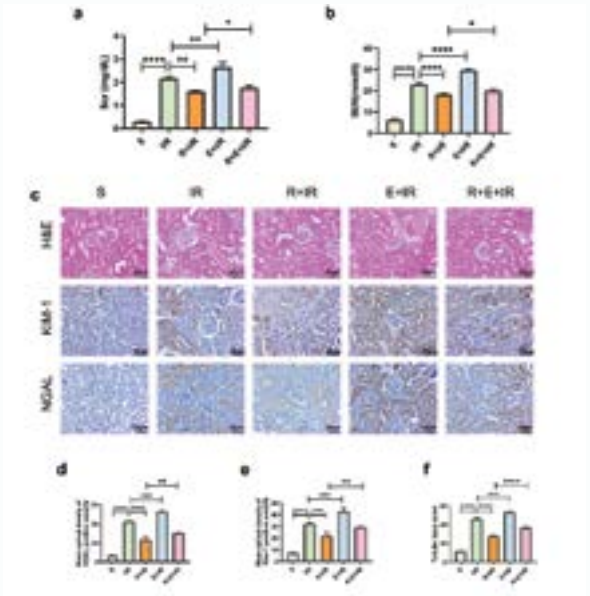

Figure 2: Renal function and renal tissue damage in each group. (a,b) Serum creatinine and urea nitrogen levels. (c) Immunohistochemical staining of renal tissue for H&E staining, Kim-1 and NGAL, images at 400× magnification, scale bar represents 20 μm. (d,e) Statistical plots of positive staining for Kim-1 and NGAL in the renal cortex. (f) Renal tubular injury score (pallerscore) analysed according to H&E staining. Data are expressed as mean ± Standard Deviation (SD) (n=3 for each group). **P<0.01, ***P<0.001. (S, IR, E+IR, W+IR, E+W+IR represent the surgery group, the I/R group, the Ruboxistaurin-treated I/R group, the Erastin-treated I/R group, and the Ruboxistaurin and Erastin combined treatment I/R group, respectively).

PKCβII inhibition reduces renal I/R-induced iron death

To elucidate the link between PKCβII and ferroptosis in renal I/R injury, we assessed ferroptosis in terms of ferroptosis-related proteins (GPX4, SLC7A1, and TFRC), biochemical indicators of ferroptosis (MDA, GSH, SOD, and Fe^{2+}), and mitochondrial damage.

Compared to the S group, the I/R group exhibited significantly lower levels of GPX4 and SLC7A11 protein expression in kidney tissues, along with significantly higher levels of TFRC protein expression (Figure 3e-h). Additionally, MDA and Fe^{2+} levels were significantly higher in the I/R group, while GSH and SOD levels were significantly lower (Figure 4a-d). The renal tubules in the I/R

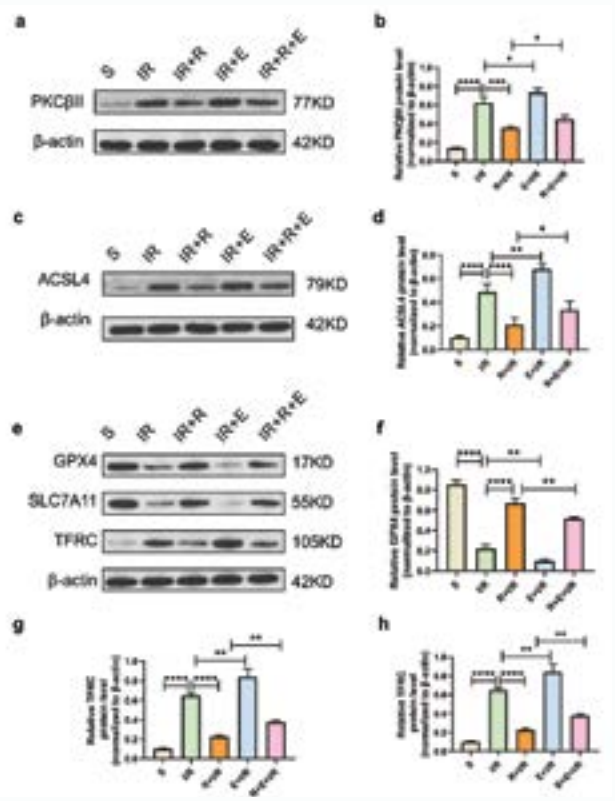

Figure 3: Expression of PKCβII, ACSL4 and iron death-associated proteins in I/R mouse models of treatment. (a) Immunoblotting of PKCβII. (b) Quantitative analysis of PKCβII protein levels. (c) ACSL4 immunoblot. (d) Quantitative analysis of ACSL4 protein levels. (e) GPX4, SLC7A11, TFRC immunoblots. (f, g, h) Quantification of GPX4, TFRC, SLC7A11 protein levels. .Data are expressed as mean ± Standard Deviation (SD) (n=3 for each group). **P<0.01, ***P<0.001. (S, IR, E+IR, W+IR, E+W+IR represent the surgery group, the I/R group, the Ruboxistaurin-treated I/R group, the Erastin-treated I/R group, and the Ruboxistaurin and Erastin combined treatment I/R group, respectively).

group displayed typical ferroptosis features, including wrinkled mitochondria, reduced cristae, and increased membrane density (Figure 4e). Following intervention with the PKCβII inhibitor Ruboxistaurin, the R+I/R group exhibited significantly higher levels of GPX4 and SLC7A11 protein expression and significantly lower levels of TFRC protein expression compared to the I/R group. Moreover, the R+I/R group showed significantly lower levels of MDA and Fe^{2+} and significantly higher levels of GSH and SOD. The mitochondria in the R+I/R group displayed improved wrinkling and significantly increased cristae. These results suggest that ferroptosis significantly increased after I/R, while it was significantly reduced after intervention with the PKCβII inhibitor Ruboxistaurin.

Inhibition of PKCβII reduces renal I/R activation of the PKCβII/ACSL4 pathway

To elucidate the potential mechanistic pathway through which PKCβII-mediated ferroptosis exacerbates renal I/R injury, our focus was on the PKCβII/ACSL4 pathway. PKCβII and ACSL4 protein expression were elevated in the I/R group compared to the S group (Figure 3a-3d). Following intervention with Ruboxistaurin, a PKCβII inhibitor, PKCβII and ACSL4 protein expression decreased in the R+I/R group compared to the I/R group.

PKCβII inhibition reduces renal I/R injury by inhibiting the

PKCβII/ACSL4 pathway to reduce iron death

To further elucidate the relationship between the PKCβII/ACSL4 pathway and ferroptosis in renal I/R, we compared the effects of the PKCβII inhibitor alone and in combination with the ferroptosis agonist Erastin. The results indicated that, compared with the R+I/R group, the E+R+I/R group exhibited significantly lower levels of GPX4 and SLC7A11 protein expression and significantly higher levels of TFRC protein expression. Furthermore, in comparison to the R+I/R group, the E+R+I/R group displayed significantly higher levels of MDA and Fe^{2+} and significantly lower levels of GSH and SOD. The mitochondria in the E+R+I/R group exhibited increased wrinkling and significantly decreased cristae compared to the R+I/R group. Additionally, the expression of PKCβII and ACSL4 protein was diminished in the E+R+I/R group compared to the R+I/R group. Notably, renal injury was more pronounced in the E+R+I/R group compared to the R+I/R group, as evidenced by elevated Scr and BUN levels, Kim-1 and NGAL expression levels, and renal tubular injury scores. These findings suggest that the inhibition of PKCβII reduces ferroptosis by inhibiting the PKCβII/ACSL4 pathway, consequently mitigating renal I/R injury.

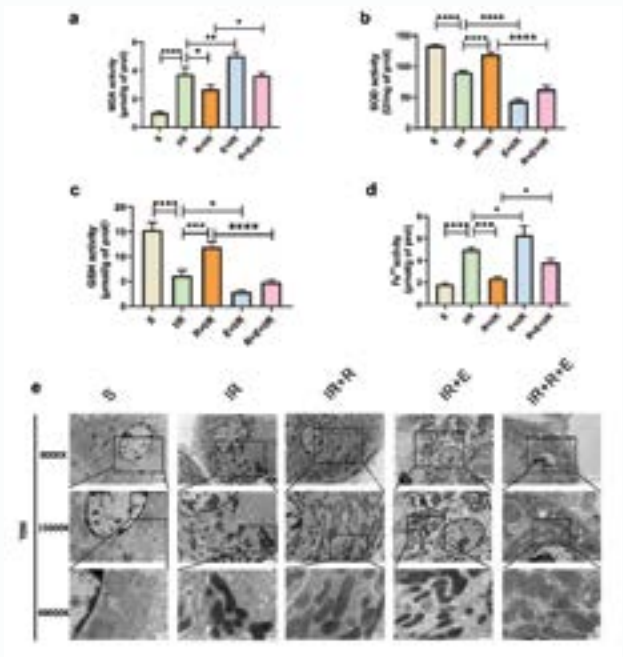

Figure 4: Changes in biochemical indicators of iron death and mitochondrial damage characteristic of iron death in the I/R mouse model of treatment. (a,b,c,d) MDA, SOD, GSH and Fe2+ levels. (e) Transmission electron microscopy showing morphological changes of mitochondria in the kidney tissue of I/R mice. Scale bars: 2 μm;1 μm; 200 nm, magnification 8000×,15000×,40000×. Data are expressed as mean ± Standard Deviation (SD) (n=3 for each group). **P<0.01, ***P<0.001. (S, IR, E+IR, W+IR, E+W+IR represent the surgery group, the I/R group, the Ruboxistaurin-treated I/R group, the Erastin-treated I/R group, and the Ruboxistaurin and Erastin combined treatment I/R group, respectively).

Discussion

In this study, we observed a significant increase in serum creatinine and urea nitrogen in renal I/R mice, an elevation in renal tubular injury score, and an upregulation in the expression of the renal injury markers KIM-1 and NGAL. These findings align with previous reports in the literature [15,16]. Additionally, we identified an increased expression of PKCβII in renal I/R injury, and the inhibition

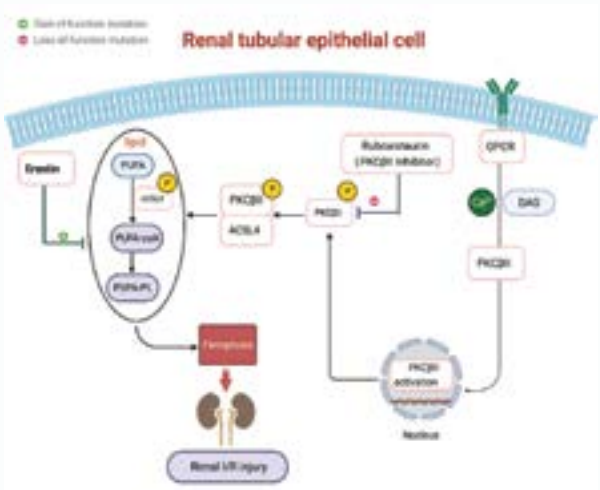

Figure 5: Possible mechanism of PKC β II-mediated iron death aggravating renal ischemia-reperfusion injury in mice.

of PKCβII successfully reversed these alterations in the indicators of renal injury. Moreover, our investigation revealed that the inhibition of PKCβII reduces ferroptosis by suppressing the PKCβII/ACSL4 pathway, thereby mitigating renal I/R injury. To our knowledge, this study is the first to demonstrate that inhibiting PKCβII can effectively reduce renal I/R injury, offering a theoretical foundation for the prevention and treatment of renal I/R injury.

The Protein Kinase C (PKC) family consists of 11 different isozymes, categorized into three groups: conventional (cPKC), novel (nPKC), and atypical (aPKC). cPKCs are activated by Diacylglycerol (DAG) and calcium ions, participating in various signaling pathways, including gene expression, cell growth, and differentiation. Numerous mechanisms have been reported to be associated with PKCβII-induced I/R protection. For instance, PKCβII mediates the phosphorylation of amino-terminal kinase in cardiac I/R injury [19]. PKCβII inhibitors protect against intestinal I/R injury in mice by inhibiting p66(Shc)-mediated oxidative stress and subsequent apoptosis [20]. The mechanism of PKCβII in liver I/R injury may involve attenuating microvascular injury, reducing the transport of injury-related factors, and decreasing the activation of NF-κB p65 [21]. Notably, the role of PKCβII in renal I/R injury has not been previously reported. Our study identified an upregulation of PKCβII in post-I/R kidneys, and the inhibition of PKCβII attenuated renal I/R injury, underscoring the significance of PKCβII as a key mediator in renal I/R injury.

Ferroptosis is a regulated form of cell demise initiated by iron-mediated lipid peroxidation, leading to the rupture of the plasma membrane and the release of damage-associated molecules [22]. Inhibition of cellular cysteine transport proteins results in the depletion of intracellular glutathione (GSH), ultimately leading to the inactivation of glutathione peroxidase (GPX4). This cascade results in the accumulation of lipid peroxidation, which, at a certain threshold, induces cell death [23]. At the cellular ultrastructural level, ferroptosis is characterized by smaller-than-normal mitochondria, wrinkling of the mitochondrial membrane, reduced or lost mitochondrial cristae, and a broken outer membrane, although morphological changes in the nucleus are not conspicuous [24]. This process is accompanied by the substantial accumulation of iron ions, heightened Reactive

Oxygen Species (ROS), and alterations in genes regulating iron homeostasis and lipid peroxidation metabolism [25]. Key regulators of iron metabolism include Transferrin Receptor (TFRC), a cell surface receptor responsible for iron import into cells [26]. Inhibition of TFRC diminishes iron input to cells, preventing the formation of ROS and the accumulation of lipid peroxides [27]. SLC7A11, located on the cell membrane, is a transporter protein that exchanges cystine for glutamate. Inhibition of SLC7A11 hampers cells' ability to synthesize GSH, leading to lipid peroxide accumulation and ferroptosis [28,29]. In our study, we investigated common ferroptosis biomarkers, encompassing cellular iron levels, lipid peroxidation products (MDA), SOD, GSH levels, and the expression of GPX4, SLC7A11, TFRC, and ACSL4. Our findings indicated a significant increase in ferroptosis in renal I/R injury, consistent with previous reports in the literature. Conversely, the inhibition of PKCβII activation markedly attenuated ferroptosis, suggesting that PKCβII may serve as a crucial mediator of ferroptosis in renal I/R.

PKCβII is potentially associated with ferroptosis, with Acyl-Coenzyme A synthase long-chain family member 4 (ACSL4) playing a crucial role. ACSL4 is a lipid-metabolizing enzyme essential for lipid peroxidation, facilitating the integration of Polyunsaturated Fatty Acids (PUFAs) onto phospholipids, which serve as a major source of peroxidized lipids. ACSL4-deficient cells exhibit significant resistance to GPX4 inhibition-induced ferroptosis [30]. Previous research by Smith identified ACSL4 as a substrate for PKC, with PKC kinase controlling its phosphorylation and, consequently, regulating its activity [31]. Zhang et al. first demonstrated the critical role of PKCβII activation in ferroptosis through a genome-wide CRISPR-Cas9 and kinase inhibitor library screen. Subsequently, PKCβII was shown to phosphorylate ACSL4, promoting its activation [32]. Activated ACSL4 significantly enhances the synthesis of phospholipids containing unsaturated fatty acids, leading to increased lipid peroxidation. This sets in motion continuous positive feedback loop of lipid peroxidation-PKCβII-ACSL4, resulting in rapid amplification of lipid peroxidation and ultimately inducing ferroptosis [33]. Additionally, some studies have reported that unsaturated carbonyl compounds in cigarette smoke gas phase affect macrophages through PKC β-dependent induction of ferroptosis [34].

In our study, we observed a significant upregulation of PKCβII and ACSL4 expression in renal I/R, and the inhibition of PKCβII effectively suppressed both. Furthermore, PKCβII inhibition reduced I/R-induced ferroptosis. However, the effects of PKCβII inhibition (inhibition of PKCβII/ACSL4 activation, reduction of ferroptosis, and mitigation of renal I/R injury) were reversed with the addition of the ferroptosis agonist Erastin. Therefore, targeted inhibition of PKCβII may hinder ferroptosis by suppressing ACSL4 expression, suggesting a potential pathway for PKCβII inhibition to alleviate renal I/R injury (Figure 5).

Our study has some limitations. Firstly, while the activation of PKCβII enhances ferroptosis and its mechanism of action is related to the regulation of the lipid peroxidation-PKCβII-ACSL4 positive feedback mechanism, the potential mechanism by which PKCβII-mediated ferroptosis exacerbates renal I/R injury remains unclear and requires further investigation. Additionally, as no in vitro experiments were conducted, this study lacks exploration of specific cells and needs to be complemented with more classical *in vitro* models of renal I/R injury (e.g., hypoxia-reoxygenation model of cells) and experimental corroboration such as ferroptosis agonist intervention or overexpression/silencing of ferroptosis-related genes. Moreover, PKCβII is a member of the PKC family, and the role of other isoforms of PKC in ferroptosis was not explored in this study.

Conclusion

In summary, this study introduces new evidence supporting the idea that inhibiting PKCβII can mitigate renal I/R injury. The observed effects appear to be mediated through the inhibition of PKCβII/ACSL4 signaling, consequently reducing ferroptosis. Hence, PKCβII emerges as a potential contributor to mediating renal I/R injury, and the targeted inhibition of PKCβII activation may offer a novel therapeutic approach to alleviate renal I/R injury. Further research is warranted to explore additional mechanisms by which PKCβII inhibition reduces ferroptosis and its protective effects on renal I/R injury.

Funding

This study was sponsored by the National Natural Science Foundation of China (82160145), the Science and Technology Fund of Guizhou Health Commission [(gzwkj2021-212) and (gzwjkj2020-1-113)], and the Guizhou Science and Technology Project [QKHZC(2021)085].

References

1. Wu Y, Shi H, Xu Y, Pei J, Song S, Chen W, et al. Ebselen ameliorates renal ischemia-reperfusion injury via enhancing autophagy in rats. Mol Cell Biochem. 2022;477(6):1873-85.
2. Li Z, Zhu J, Wan Z, Li G, Chen L, Guo Y. Theaflavin ameliorates renal ischemia/reperfusion injury by activating the Nrf2 signalling pathway in vivo and in vitro. Biomed Pharmacother. 2021;134:111097.
3. Mochly-Rosen D, Das K, Grimes KV. Protein kinase C, an elusive therapeutic target? Nat Rev Drug Discov. 2012;11(12):937-57.
4. Newton AC. Protein kinase C: perfectly balanced. Crit Rev Biochem Mol Biol. 2018;53(2):208-30.
5. Kalogeris T, Baines CP, Krenz M, Korthuis RJ. Cell biology of ischemia/reperfusion injury. Int Rev Cell Mol Biol. 2012;298:229-317.
6. Padanilam BJ. Induction and subcellular localization of protein kinase C isozymes following renal ischemia. Kidney Int. 2001;59(5):1789-97.
7. Ralhan I, Chang J, Moulton MJ, Goodman LD, Lee NYJ, Plummer G, et al. Autolysosomal exocytosis of lipids protect neurons from ferroptosis. J Cell Biol. 2023;222(6):e202207130.
8. Granata S, Votrico V, Spadaccino F, Catalano V, Netti GS, Ranieri E, et al. Oxidative Stress and Ischemia/Reperfusion Injury in Kidney Transplantation: Focus on Ferroptosis, Mitophagy and New Antioxidants. Antioxidants (Basel). 2022;11(4):769.
9. Fujita T, Asai T, Andrassy M, Stern DM, Pinsky DJ, Zou YS, et al. PKCbeta regulates ischemia/reperfusion injury in the lung. J Clin Invest. 2004;113(11):1615-23.
10. Al-Onazi AS, Al-Rasheed NM, Attia HA, Al-Rasheed NM, Ahmed RM, Al-Amin MA, et al. Ruboxistaurin attenuates diabetic nephropathy via modulation of TGF-β1/Smad and GRAP pathways. J Pharm Pharmacol. 2016;68(2):219-32.
11. Zhao J, Xu B, Xiong Q, Feng Y, Du H. Erastin-induced ferroptosis causes physiological and pathological changes in healthy tissues of mice. Mol Med Rep. 2021;24(4):713.
12. Zhang X, Li LX, Ding H, Torres VE, Yu C, Li X. Ferroptosis Promotes Cyst Growth in Autosomal Dominant Polycystic Kidney Disease Mouse Models. J Am Soc Nephrol. 2021;32(11):2759-76.
13. Li Q, Wang Z, Zhang Y, Zhu J, Li L, Wang X, et al. NLRC5 deficiency protects against acute kidney injury in mice by mediating carcinoembryonic antigen-related cell adhesion molecule 1 signaling. Kidney Int. 2018;94(3):551-66.
14. Paller MS, Hoidal JR, Ferris TF. Oxygen free radicals in ischemic acute renal failure in the rat. J Clin Invest. 1984;74(4):1156-64.

15. Chen C, Wang D, Yu Y, Zhao T, Min N, Wu Y, et al. Legumain promotes tubular ferroptosis by facilitating chaperone-mediated autophagy of GPX4 in AKI. Cell Death Dis. 2021;12:65.

16. Viñas JL, Spence M, Gutsol A, Knoll W, Burger D, Zimpelmann J, et al. Receptor-Ligand Interaction Mediates Targeting of Endothelial Colony Forming Cell-derived Exosomes to the Kidney after Ischemic Injury. Sci Rep. 2018;8(1):16320.

17. Nishizuka Y. Protein kinase C and lipid signaling for sustained cellular responses. FASEB J. 1995;9(7):484-96.

18. Singh RK, Kumar S, Tomar MS, Verma PK, Singh SP, Gautam PK, et al. Classical Protein Kinase C: a novel kinase target in breast cancer. Clin Transl Oncol. 2019;21(3):259-67.

19. Kong L, Andrassy M, Chang JS, Huang C, Asai T, Szabolcs MJ, et al. PKCbeta modulates ischemia-reperfusion injury in the heart. Am J Physiol Heart Circ Physiol. 2008;294(4):H1862-70.

20. Wang G, Chen Z, Zhang F, Jing H, Xu W, Ning S, et al. Blockade of PKCβ protects against remote organ injury induced by intestinal ischemia and reperfusion via a p66shc-mediated mitochondrial apoptotic pathway. Apoptosis. 2014;19(9):1342-53.

21. Meng GX, Yuan Q, Wei LP, Meng H, Wang YJ. Protein kinase C-β inhibitor treatment attenuates hepatic ischemia and reperfusion injury in diabetic rats. Exp Ther Med. 2016;11(2):565-70.

22. Wahida A, Conrad M. Ferroptosis: Under pressure! Curr Biol. 2023;33(7):R269-R272.

23. Wu L, Xian X, Tan Z, Dong F, Xu G, Zhang M, et al. The Role of Iron Metabolism, Lipid Metabolism, and Redox Homeostasis in Alzheimer's Disease: from the Perspective of Ferroptosis. Mol Neurobiol. 2023;60(5):2832-50.

24. Wang H, Liu C, Zhao Y, Gao G. Mitochondria regulation in ferroptosis. Eur J Cell Biol. 2020;99(1):151058.

25. Yang WS, Stockwell BR. Ferroptosis: Death by Lipid Peroxidation. Trends Cell Biol. 2016;26(3):165-76.

26. MacKenzie EL, Iwasaki K, Tsuji Y. Intracellular iron transport and storage: from molecular mechanisms to health implications. Antioxid Redox Signal. 2008;10(6):997-1030.

27. Yu H, Yang C, Jian L, Guo S, Chen R, Li K, et al. Sulfasalazine-induced ferroptosis in breast cancer cells is reduced by the inhibitory effect of estrogen receptor on the transferrin receptor. Oncol Rep. 2019;42(2):826-38.

28. Parker JL, Deme JC, Kolokouris D, Kuteyi G, Biggin PC, Lea SM, et al. Molecular basis for redox control by the human cystine/glutamate antiporter system xc. Nat Commun. 2021;12(1):7147.

29. Lang X, Green MD, Wang W, Yu J, Choi JE, Jiang L, et al. Radiotherapy and Immunotherapy Promote Tumoral Lipid Oxidation and Ferroptosis via Synergistic Repression of SLC7A11. Cancer Discov. 2019;9(12):1673-85.

30. Gan B. ACSL4, PUFA, and ferroptosis: new arsenal in anti-tumor immunity. Signal Transduct Target Ther. 2022;7(1):128.

31. Smith ME, Saraceno GE, Capani F, Castilla R. Long-chain acyl-CoA synthetase 4 is regulated by phosphorylation. Biochem Biophys Res Commun. 2013;430(1):272-7.

32. Zhang HL, Hu BX, Li ZL, Du T, Shan JL, Ye ZP, et al. PKCβII phosphorylates ACSL4 to amplify lipid peroxidation to induce ferroptosis. Nat Cell Biol. 2022;24(1):88-98.

33. Lei G, Horbath A, Li Z, Gan B. PKCβII-ACSL4 pathway mediating ferroptosis execution and anti-tumor immunity. Cancer Commun (Lond). 2022;42(7):583-6.

34. Higashi T, Handa H, Mai Y, Maenaka K, Tadokoro T. Protein kinase Cβ is involved in cigarette smoke gas phase-induced ferroptosis in J774 macrophages. J Pharmacol Sci. 2023;153(1):22-5.